



HAL
open science

Quantitation of imidazo[1,2- a]quinoxaline derivatives in human and rat plasma using LC/ESI-MS

Sonia Khier, Georges Moarbess, Carine Deleuze-Masquéfa, Isabelle Solassol, Delphine Margout, Frédéric Pinguet, Pierre-Antoine Bonnet, Françoise Bressolle

► To cite this version:

Sonia Khier, Georges Moarbess, Carine Deleuze-Masquéfa, Isabelle Solassol, Delphine Margout, et al.. Quantitation of imidazo[1,2- a]quinoxaline derivatives in human and rat plasma using LC/ESI-MS. Journal of Separation Science, 2009, 32 (9), pp.1363-1373. 10.1002/jssc.200800668 . hal-02309624

HAL Id: hal-02309624

<https://hal.science/hal-02309624>

Submitted on 9 Oct 2019

HAL is a multi-disciplinary open access archive for the deposit and dissemination of scientific research documents, whether they are published or not. The documents may come from teaching and research institutions in France or abroad, or from public or private research centers.

L'archive ouverte pluridisciplinaire **HAL**, est destinée au dépôt et à la diffusion de documents scientifiques de niveau recherche, publiés ou non, émanant des établissements d'enseignement et de recherche français ou étrangers, des laboratoires publics ou privés.

Sonia Khier¹
Georges Moarbess^{2*}
Carine Deleuze-Masquefa^{2*}
Isabelle Solassol³
Delphine Margout¹
Frédéric Pinguet³
Pierre-Antoine Bonnet²
Françoise M. M. Bressolle¹

Original Paper

Quantitation of imidazo[1,2-*a*]quinoxaline derivatives in human and rat plasma using LC/ESI-MS

¹Clinical Pharmacokinetic Laboratory, EA4215, Faculty of Pharmacy, University Montpellier I, France
²Pharmacochemistry and Biomolecule Laboratory, EA4215, Faculty of Pharmacy, University Montpellier I, France
³Department of Oncopharmacology, Pharmacy service, Val d'Aurelle Anticancer Centre, Parc Euromédecine, France

Since several years, our group developed quinoxalinic compounds. Among the synthesized compounds, in the imidazo[1,2-*a*]quinoxaline series, EAPB0203 has shown interesting activities both on melanoma and lymphoma. The structure of EAPB0203 has been modulated and a new compound, EAPB0503, exhibits an *in vitro* cytotoxic activity on melanoma cancer cell line 7–9 times higher than EAPB0203. We validated an LC/ESI-MS method to simultaneously quantify EAPB0503 and its metabolite EAPB0603 in human and rat plasma. Chromatography was performed on a C8 Zorbax eclipse XDB column with a mobile phase consisting of acetonitrile and formate buffer gradient elution. LC-MS data were acquired in SIM mode at *m/z* 305, 291, and 303 for EAPB0503, EAPB0603, and the internal standard, respectively. The drug/internal standard peak area ratios were linked *via* quadratic relationships to concentrations (low range: 5–300 µg/L, high range: 100–1000 µg/L). The method is precise (precision, ≤14%) and accurate (recovery, 92–113%). Mean extraction efficiencies, >72% for each analyte, were obtained. The lower LOQs were 5 µg/L. This highly specific and sensitive method was successfully used to investigate plasma concentrations of EAPB0503 and EAPB0603 in a pharmacokinetic study carried out in rat and would also be useful in clinical trials at a later stage.

Keywords: Human and rat matrices / Imidazo[1,2-*a*]quinoxaline / LC/ESI-MS / Lymphoma / Melanoma

Received: November 20, 2008; revised: January 22, 2009; accepted: January 22, 2009

DOI 10.1002/jssc.200800668

2 Experimental

2.1 Chemicals and reagents

2.2 Instrumentation

2.3 Sample preparation

2.4 Method validation

2.5 Application

1 Introduction

Imiquimod (S-26308, R-837) (1-(2-methylpropyl)-1*H*-imidazo[4,5-*c*]quinolin-4-amine), the first member of the imidazoquinolone family, belongs to the class of medications called immune response modifiers. This compound has potent antiviral and antitumor activity *in vivo*. Imiquimod is used in the topical treatment of genital and anal warts by increasing the activity of the body's immune system [1–3]. This drug is also efficacious as a topical therapy for certain types of skin cancers: basal cell carcinoma, Bowen's disease, superficial squamous cell carcinoma, some superficial malignant melanomas, and actinic keratosis [4–6]. Imiquimod inhibits melanogenesis and proliferation of human melanocytes [7]. Recently, its therapeutic

spectrum was extended to cutaneous B-cell lymphomas [8]. The exact mechanism of action in which imiquimod and its analogs activate the immune system is not yet known. Nevertheless, it is known that imiquimod activates immune cells by ligating the Toll-like receptor 7 (TLR7), commonly involved in pathogen recognition, on the cell surface [9]. Cells activated by imiquimod *via* TLR-7 secrete cytokines (primarily interferon- α (IFN- α), interleukin-6 (IL-6), and tumor necrosis factor- α (TNF- α) [10]. There is evidence that imiquimod, when applied to skin, can lead to the activation of Langerhans cells, which subsequently migrate to local lymph nodes to activate the adaptive immune system [11]. Other cell types activated by imiquimod include natural killer cells, macrophages, and B-lymphocytes [11]. Imiquimod also has direct *in vitro* and *in vivo* pro-apoptotic activities in a rather tumor selective manner [9, 12, 13].

Since several years, our group has developed analogues of imiquimod. Three chemical series have been synthesized [14]: i) the imidazo[1,2-*a*]quinoxalines, ii) the imidazo[1,5-*a*]quinoxalines, and iii) the pyrazolo[1,5-*a*]qui-

Correspondence: Dr. Françoise M. M. Bressolle, Laboratoire de Pharmacocinétique Clinique, EA4215, Faculté de Pharmacie, 15 Avenue Ch. Flahault, Université Montpellier I, 34093 Montpellier Cedex 5, France
E-mail: fbressolle@aol.com
Fax: (+33)-4-67-54-80-75

Abbreviations: IC₅₀, 50% inhibitory concentration; SPE, solid phase extraction; QC, quality control

* These two authors contributed equally to this work.

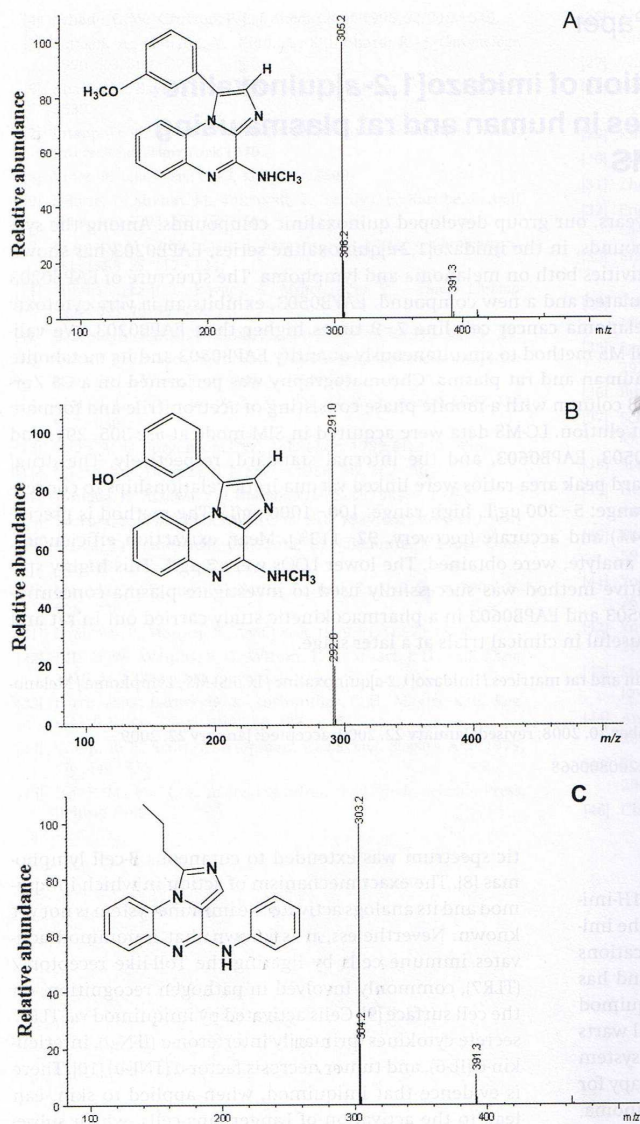


Figure 1. Mass spectra (scan mode) of EAPB0503 (A), EAPB0603 (B), and internal standard (C).

noxalines. Among the imidazo[1,2-*a*]quinoxaline series, we recently demonstrated that one of these compounds (EAPB0203) induced inhibition of cell proliferation and apoptosis in HTLV-I transformed and HTLV-I-negative malignant T-cells as well in fresh adult T-cell leukaemia (ATL) cells [15]. This compound exhibits inhibition of cell proliferation, G2/M cell cycle arrest, and induction of apoptosis in HTLV-I transformed and HTLV-I negative malignant T-cells while normal resting or activated T lymphocytes are resistant. Furthermore, EAPB0203 almost completely inhibited the growth of freshly iso-

lated ATL cells at concentrations of 1 to 10 μ M. EAPB0203 treatment significantly down-regulated the anti-apoptotic proteins c-IAP-1 and Bcl-XL, and resulted in a significant loss of mitochondrial membrane potential, cytoplasmic release of cytochrome c, and caspase dependent apoptosis. In addition, in HTLV-I transformed cells only, EAPB0203 treatment stabilized p21 and p53 proteins but had no effect on NF- κ B activation [15].

EAPB0203 also has a potential therapeutic role in the treatment of malignant melanoma [16]. In a mouse model, EAPB0203 treatment schedules caused a signifi-

cant decrease in tumor size compared to vehicle control and fotemustine treatment [16]. The chemical structure of this lead molecule has been modulated to optimize its effect [17]. Among the new synthesized compounds, one of them, EAPB0503, (Fig. 1a, 50% inhibitory concentration, $IC_{50} = 200 \pm 90$ nM), has 7–9 times higher cytotoxic activity against human melanoma cell line (A375) than EAPB0203 ($IC_{50} = 1.57 \pm 0.56$ μ M).

In this paper, we describe an LC/ESI-MS method to simultaneously quantify EAPB0503 and EAPB0603 (Fig. 1b) in human and rat plasma. EAPB0603, in which the methoxy group has been replaced by a hydroxyl function, could be a possible metabolite of EAPB0503 in the body. The preparation of the sample was based on a solid-phase extraction procedure of plasma samples in the presence of an internal standard belonging to the imidazo[1,5-*a*]quinoxaline series (Fig. 1c). The developed and validated analytical method was applied to quantify EAPB0503 and EAPB0603 in plasma samples obtained during a pharmacokinetic study in rats.

2 Experimental

2.1 Chemicals and reagents

EAPB0503 (1-(3-methoxyphenyl)-*N*-methylimidazo[1,2-*a*]quinoxalin-4-amine; molecular weight, 304), EAPB0603 (1-(3-hydroxyphenyl)-*N*-methylimidazo[1,2-*a*]quinoxalin-4-amine; molecular weight, 290), and the internal standard (*N*-phenyl-1-propylimidazo[1,5-*a*]quinoxalin-4-amine; molecular weight, 302) (Fig. 1) were synthesized by the Pharmacochemistry and Biomolecule Laboratory (EA 4215, Montpellier I University) [14]. The purity of these standards was evaluated by elemental analysis and RMN. They were stored at 20°C protected from light. TFA was purchased from Sigma (St. Louis, MO, USA). Acetonitrile and dichloromethane (HPLC grade) were obtained from Carlo Erba (Val de Reuil, France). Ammonium formate was from Fluka (Vandoeuvre, France) and formic acid from Prolabo (Paris, France). All chemicals were of the highest purity available. Oasis HLB cartridges (30 mg of sorbent, average particle diameter 30 μ m) were supplied by Waters (Saint Quentin, France). Drug-free Caucasian human plasma samples (six different batches from six different pools of donors) were obtained from the Etablissement Français du Sang (Montpellier, France). Drug-free rat plasma (six different batches obtained from pooled rat plasma) was obtained from healthy male Sprague Dawley rats (weight, 230–270 g) provided from Charles River (L'Arbresle Cedex, France). These plasma pools were obtained from blood collected on lithium heparinate to prevent coagulation. Blank matrices were aliquoted and stored at -80°C until used. Formate buffer pH 3 was prepared by dissolving 126 mg of ammonium formate in 1 L of purified water; the pH was adjusted

with formic acid. Purified water was generated by a Milli-Q reagent water system (Millipore, Bedford, MA, USA).

Two stock solutions (A and B) of EAPB0503 and EAPB0603 (40 mg/L) and of the internal standard (20 mg/L) were prepared in a mixture of acetonitrile–water–formic acid (49.5:49.5:1, v/v/v). Extemporaneous dilutions of each stock were made with acetonitrile–water–formic acid as appropriate to prepare working solutions (from 0.125 to 25 mg/L). Dilutions of stock A were used in the preparation of the calibration curves and dilutions of stock B were used in the preparation of quality control (QC) samples. These stock solutions were stored at $+4^{\circ}\text{C}$ for 2 months.

2.2 LC-MS analyses

LC-MS experiments were carried on a Hewlett Packard Agilent 1100 quadrupole mass spectrometer (Agilent Technologies, Les Ulis, France), working with an electrospray ionization source (ESI). The mass spectrometer was coupled to a Hewlett Packard LC system equipped with a quaternary pumping unit, a degasser, and an autosampler with a loading valve fitted with a 100 μ L loop and set at 4°C . HPChem software (version 08.04) from Agilent Technologies was used for system control, data acquisition, and data analysis. The mass spectrometer was tuned with the procedures provided by Agilent Technologies to give a maximum response for m/z 118, 230, 508, and 997. The ESI-MS signal was then optimized during continuous infusion of a solution of the three analytes (EAPB0503, EAPB0603, and internal standard), at the concentrations of 5 mg/L, dissolved in the acetonitrile–water–formic acid mixture. The use of an acidic solution to dissolve the analytes favors ionization. Optimized parameters were as follows: i) heated N_2 gas of 350°C and 12 L/min was used to evaporate solvent from the electrospray chamber, ii) compressed N_2 gas of 35 psi was used for nebulization, and iii) voltage was set at +3.0 kV for the capillary. The intensity of $[\text{M} + \text{H}]^+$ increased as the sampling cone voltage increased from 25 to 80 (EAPB0603) or 100 V (EAPB0503 and internal standard) and decreased significantly when it passed 80–100 V. Thus, for the rest of the study, the sampling cone voltage was set at 80 V for EAPB0603, and 100 V for EAPB0503 and the internal standard. The mass spectrometer was operated at positive mode and mass spectra were collected in scan mode (m/z 100–500). For quantitative measurement of EAPB0503 and EAPB0603, SIM was employed.

Chromatographic conditions were optimized to obtain sharp peak shape with adequate response. This included column type (C8, C18, phenyl or Shield RP18), composition of the mobile phase, pH of buffer solution and flow rate. The presence of organic acid (formic, acetic, or trifluoroacetic acid) or buffer (formate or acetate) in the mobile phase was evaluated.

Using the C18 or Shield RP18 column, analytes were too retained due to hydrophobic interactions, while using the phenyl column poor selectivity was observed. Best separations of the analytes and relative short analysis time were obtained on a C8 Zorbax eclipse XDB (150 × 4.6 mm id; 5 μm particle size, Agilent Technologies) using a mobile phase consisting of eluent A, acetonitrile, and eluent B, 2 mM ammonium formate buffer. The starting eluent was 30% A and 70% B after which the proportion of eluent A was increased linearly to 100% in 9 min then held for 1 min in order to wash the column, returned to initial composition of eluent A (30%) and B (70%) in 1 min and then held for 3 min in order to re-equilibrate the column. The analytical column was linked to a filter insert assay (Waters). The column temperature was 20°C. Chromatography was carried out at flow rate of 0.8 mL/min. The injection volume was 10 μL.

2.3 Sample preparation

In the initial step, it was searched for the most important variables to optimize the extraction efficiency of the analytes in the solid phase extraction (SPE) clean up. These following variables were included in this screening design: i) the acid used to precipitate proteins before SPE (formic acid or TFA), ii) the nature of the SPE sorbent (silica based-sorbents: C8, C18, phenyl or polymeric sorbents: Oasis® HLB or Strata™X), ii) the nature and the amount of washing solvent (water with or without 1–2% methanol), and iii) the composition of eluting solvent (acetonitrile, methanol, or chloroform) and speed of the elution process. In a second step, the best conditions were slightly modified to obtain a good selectivity in regard to endogenous compounds from the matrix. Different internal standards from this new group of compounds were also checked. Finally, the optimized sample pretreatment was as follows: to 0.5 mL of plasma sample, 20 μL of the internal standard solution (1 mg/L for low calibration curves; 5 mg/L for high calibration curves) and 0.5 mL of water containing 10 mL/L TFA were added. The mixture was centrifuged at 4000 × g for 10 min at 4°C. The supernatant was applied onto an Oasis HLB cartridge previously conditioned with 1 mL of methanol and 1 mL purified water. The cartridge was then washed with 1 mL of water and then the analytes were eluted with 2 × 1 mL dichloromethane. The eluate was evaporated to dryness under nitrogen at 40°C. The residue was dissolved in 100 μL of the mixture containing acetonitrile–water–formic acid (49.5:49.5:1, v/v/v).

2.4 Preparation of calibration curves and QC samples

Drug-free plasma (from human or rat) was spiked with appropriate working solutions of EAPB0503 and

EAPB0603 to provide two calibration curves: the first one in the range 5 to 300 μg/L, and the second one from 100 to 1000 μg/L. From recorded peak areas, the ratios of each analyte to internal standard were calculated. To link peak area ratios and theoretical concentrations of each analyte, different models were tested: i) unweighted or weighted least-squares linear regression analysis ($Y = aX + b$) and ii) quadratic relationship ($Y = aX^2 + bX + c$) with Y = peak area ratio and X = nominal concentration. The regression curve was not forced through zero. The resulting equation parameters were used to back calculate concentrations for the calibrators that were statistically evaluated.

QC samples were prepared in the same way by spiking drug-free matrix with working solutions to provide low, medium, and high concentrations: 15, 75, 200, 300, 500, and 750 μg/L. QC samples were used during the study to determine extraction efficiencies, and accuracy and precision of the method as well as to perform stability assays.

2.5 Matrix effect and selectivity

The matrix effect (*i.e.*, suppression or enhancement of ionization of analytes by the presence of matrix components) was assessed by calculating the matrix factor [18]. It was defined as a ratio of the analyte peak response in the presence of matrix ions to the analyte peak response in the absence of matrix ions. It was performed by processing six individual lots of each drug-free matrix as described above. The dried extracts were reconstituted with 100 μL of the water–acetonitrile–formic acid mixture containing EAPB0503 and EAPB0603 at the concentrations of QC samples and the internal standard at the concentration of 0.04 or 0.2 mg/L. Each determination was replicated eight-fold. Reference solutions were prepared in the formic acid–acetonitrile–water mixture at the same nominal concentrations ($n = 3$ per concentration). The reconstituted extracts and reference solutions were injected onto the analytical column. Peak areas of the analytes in the extracted samples were compared with those in the references (injected five-fold). Matrix factor values between 0.85–1.15 were judged acceptable.

We evaluated the selectivity of the method by running drug-free plasma samples from six different pools and by examining the chromatograms for visible evidence of interfering endogenous compounds with the compounds of interest.

2.6 Method validation

The within-day and between-day precision and accuracy of the method were validated by analyzing QC samples against a calibration curve. Determinations were performed with six replicates per QC on the same day as

well as each day for 8–17 separate days. In order to test whether it was possible to apply the described method to samples whose rat plasma concentrations were higher than the last calibration point, a QC sample containing 2400 µg/L of EAPB0503 and 1600 µg/L of EAPB0603 was prepared, diluted five-fold with blank drug-free rat plasma in order to bring concentration within the range of calibration curve and analyzed six times against a calibration curve. The CV served as the measure of precision. The accuracy was evaluated by means of recovery assays and was calculated as [mean found concentration/nominal concentration] × 100.

The absolute extraction efficiencies for EAPB0503 and EAPB0603 were determined based on the comparison of the peak areas of extracted QC samples with those obtained by direct injections of the same amount of both compounds ($n = 3$ per concentration) dissolved in the acetonitrile–water–formic acid mixture. The extraction efficiency of the internal standard was also calculated.

The lower LOQ was defined as the lowest drug concentration that could be determined with a precision $\leq 20\%$ and a recovery of 80–120%.

2.7 Stability assays

The stability of EAPB0503 and EAPB0603 in frozen plasma samples (-80°C), and in processed samples left at room temperature (20°C) and at 4°C in the refrigerator over 6 h was studied at the concentrations of QC samples. The freeze–thaw stability was evaluated for two cycles of thawing at room temperature followed by re-freezing to -80°C for 24 h. QC samples were analyzed against a calibration curve immediately after preparation (reference values) then after storage. Each determination was performed in triplicate. A drug was considered stable if at least 85% of the intact drug was retained at the end of the study period. The potential influence of the evaporating step was also tested. Run-time stability of processed samples in the autosampler was determined at 4°C for 48 h for each calibration point.

2.8 Hematological toxicity and pharmacokinetic study

This research adhered to the “Principles of Laboratory Animal Care” (NIH publication (#85-23, revised 1985). The animal study was approved by the local animal use committee.

Rats were randomly distributed in three experiment groups. In the first group, five rats received intravenous administrations of EAPB0503 (3 mg/kg dissolved in 100 µL DMSO) into the tail vein, once a day for five consecutive days. This dose was chosen according to the 50% lethal dose in rat, 8 mg/kg. In the second group, 3 rats received the vehicle (100 µL DMSO) once a day for 5 con-

secutive days. The last group corresponds to three untreated rats (control group). All rats were examined at least twice a day so as to record any signs of ill-health or behavioral changes. The bodyweight was controlled daily; the quantity of food and tap water consumed was measured daily. To evaluate possible bone marrow toxicity, blood samples (0.5 mL, collected in EDTA polypropylene tubes) were drawn by cardiac puncture just prior to drug administration, then 4 and 7 days after the beginning of treatment. The following hematological parameters, platelet count, red blood cells count, white blood cells count, hemoglobin and hematocrit, were determined.

The method was used to quantify EAPB0503 and EAPB0603 in Sprague Dawley rat plasma following single intravenous administrations of 5 mg/kg of EAPB0503 into the penis vein. Blood samples (one sample *per* rat) were drawn in heparinized polypropylene tubes at the following time-points (three animals *per* time-point), before administration, then 5, 10, 30 min, and 1, 2, 4, 8, 12, 24, and 36 h after drug administration. Blood samples were collected after sacrifice of the animal by section of the carotid artery. Two minutes prior to sampling, animals were anaesthetized with sevoflurane. Blood samples were centrifuged at 4°C ($4000 \times g$ for 10 min). Plasma samples were transferred into polypropylene tubes and stored at -80°C until assay.

Pharmacokinetic parameters were calculated by compartmental analysis from the average concentration values at each time point using the Pk-fit software [19, 20].

3 Results

3.1 Mass spectra and chromatography

From the full-scan spectra (Fig. 1), EAPB0503 and EAPB0603 were evidenced by the protonated molecules, $[M + H]^+$, at m/z 305.2 and 291, respectively. The internal standard was characterized by the protonated molecule $[M + H]^+$ at m/z 303.2. The representative chromatograms in Fig. 2A–C show drug-free human plasma spiked with EAPB0503 and EAPB0603 at the lower LOQ, drug-free rat plasma spiked with the two analytes at the lower LOQ, and rat plasma obtained 5 min after intravenous administration of EAPB0503 (5 mg/kg), respectively. The retention times of EAPB0503, EAPB0603 and internal standard were 6.7, 4.5, and 8.6 min, respectively (CVs, 1.0–2.3%, $n = 30$). For both EAPB0503 and EAPB0603, quadratic calibration curves gave the best fit based on the statistical analysis results [21] and precision and recovery of QC samples. CV values on the slope b were $<30\%$ in human and rat plasma (Table 1). Mean back calculated concentrations are presented in Tables 2 and 3. For each analyte and for each matrix, the goodness of fit between back calculated concentrations and nominal concentrations was

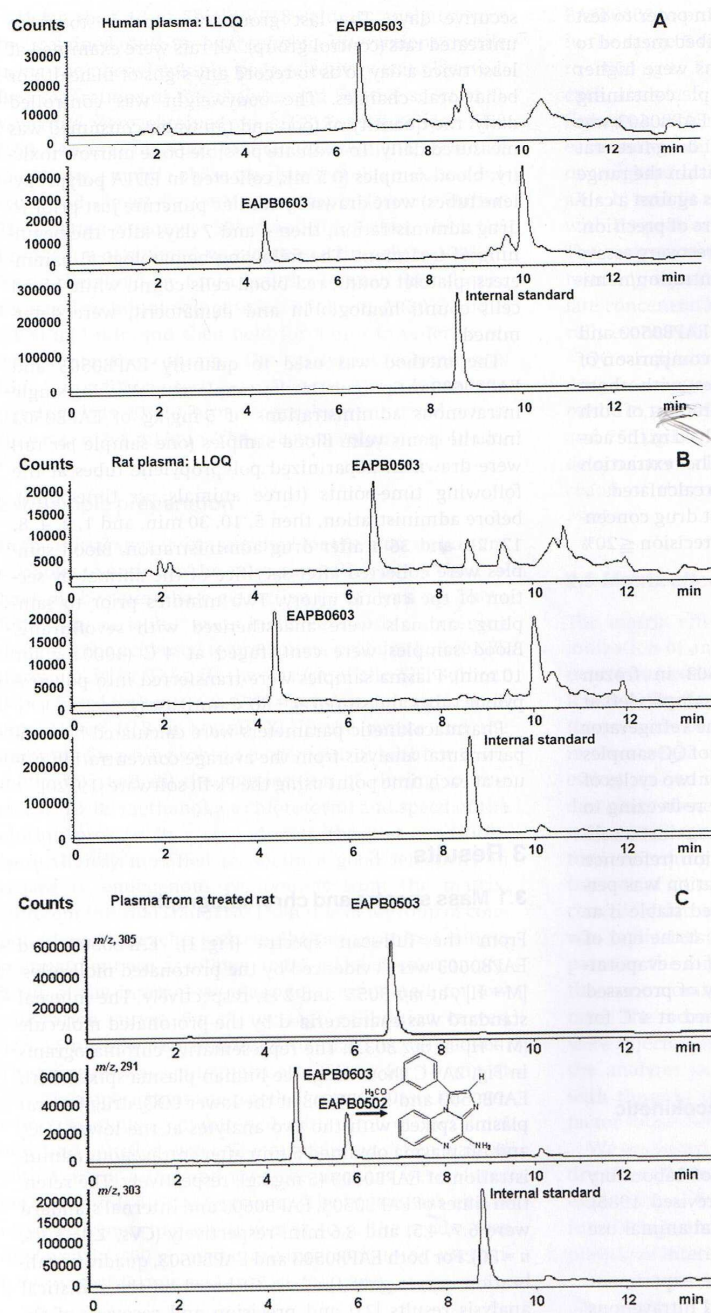


Figure 2. Typical chromatograms of drug-free plasma spiked with EAPB0503 and EAPB0603 at the LLOQ: (A) human plasma; (B) rat plasma; and chromatogram of a treated rat 5 min after EAPB0503 administration of 5 mg/kg; (C): EAPB0503, 3.0 mg/L; EAPB0603, 0.113 mg/L. Under the same chromatographic conditions, a second metabolite (EAPB0502) of EAPB0503 was detected at m/z 291. It was formed after loss of the methyl moiety on the aminomethyl group. For LC-MS conditions see instrumentation section.

statistically verified (Student's *t*-test). The mean relative predictor error calculated from the difference between back calculated and nominal concentrations was not statistically different from zero.

3.2 Validation

The six different lots of human and rat plasma, commercially procured, were chromatographically screened for interfering substances and did not show significant

Table 1. Mean parameters of the quadratic equation ($Y = aX^2 + bX + c$)

	EAPB0503	EAPB0603	EAPB0503	EAPB0603
	Low calibration curves		High calibration curves	
Human plasma				
Within day (n = 6)				
a	-1.15×10^{-5}	-5.97×10^{-6}	-1.48×10^{-6}	-5.95×10^{-7}
b	1.55×10^{-2} (19.8%)	8.08×10^{-3} (17.7%)	3.72×10^{-3} (14.3%)	1.76×10^{-3} (10.3%)
c	-8.00×10^{-3}	-8.98×10^{-3}	7.68×10^{-2}	7.61×10^{-2}
Between-day (n = 17)				
a	-1.47×10^{-5}	-4.73×10^{-6}	-9.76×10^{-7}	-1.15×10^{-6}
b	1.85×10^{-2} (21.1%)	7.48×10^{-3} (27.9%)	3.41×10^{-3} (14.9%)	2.97×10^{-3} (28.8%)
c	1.03×10^{-2}	5.02×10^{-3}	1.56×10^{-1}	7.67×10^{-3}
Rat plasma				
Between-day (n = 8)				
a	-6.11×10^{-6}	-4.09×10^{-6}	-6.36×10^{-7}	-2.14×10^{-7}
b	1.33×10^{-2} (29.5%)	7.22×10^{-3} (13.8%)	3.04×10^{-3} (11.5%)	1.43×10^{-3} (21.4%)
c	1.35×10^{-2}	1.09×10^{-2}	1.01×10^{-1}	3.65×10^{-2}

CVs are given between parentheses.

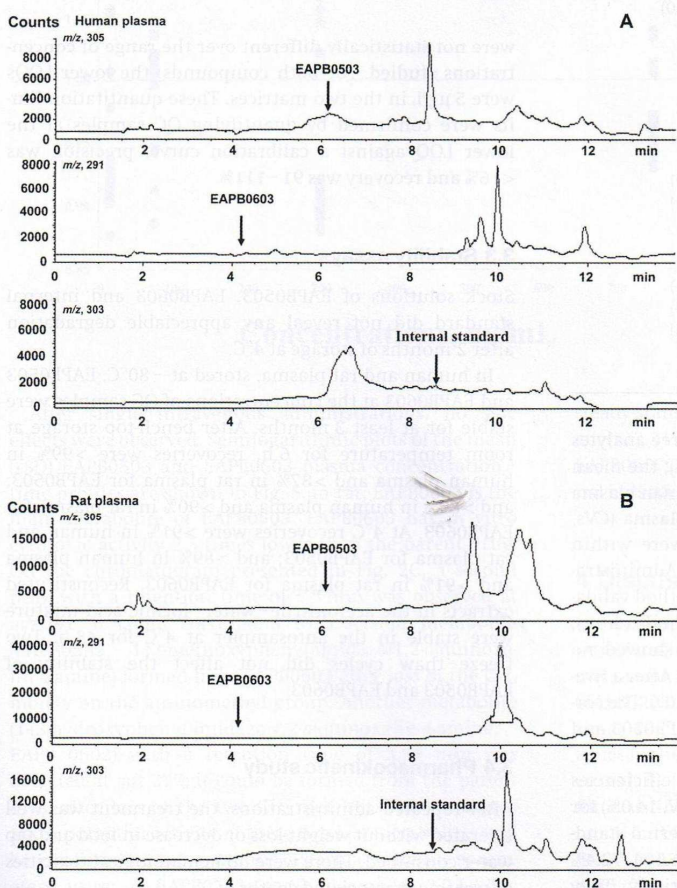


Figure 3. Chromatograms of blank human (A) and rat (B) plasma. For LC-MS conditions see instrumentation section.

Table 2. CVs and recoveries, calculated from back calculated concentrations, from calibration curves performed in human plasma

Nominal concentrations ($\mu\text{g/L}$)	CV, % (Recovery, %)	
	EAPB0503	EAPB0603
Low calibration curves		
Within-day ($n = 6$)		
5	13 (105)	8.3 (109)
7.5	5.5 (111)	7.9 (107)
10	6.0 (99)	6.1 (102)
20	3.8 (93)	8.7 (91)
50	9.9 (97)	5.0 (102)
100	1.6 (100)	1.8 (99)
300	0.24 (100)	0.70 (100)
Between-day ($n = 17$)		
5	9.8 (100)	11 (91)
7.5	6.4 (103)	9.0 (104)
10	5.4 (97)	7.0 (98)
20	5.7 (100)	8.9 (101)
50	6.7 (100)	4.6 (101)
100	4.4 (99)	5.8 (98)
300	2.5 (100)	0.58 (100)
High calibration curves		
Within-day ($n = 6$)		
100	5.7 (103)	2.7 (93)
150	11 (98)	3.5 (98)
400	1.9 (106)	4.3 (106)
600	3.9 (97)	2.3 (96)
800	8.6 (100)	8.2 (104)
1000	7.0 (100)	2.9 (103)
Between-day ($n = 17$)		
100	6.0 (94)	7.2 (95)
150	14 (103)	5.6 (104)
400	2.5 (100)	6.0 (100)
600	9.9 (101)	4.2 (100)
800	9.4 (96)	5.2 (99)
1000	7.7 (100)	5.5 (98)

interference at the retention times of the three analytes (Fig. 3). No matrix effect was observed (Fig. 4); the mean matrix factors ranged from 88 to 101% in human plasma (CVs, 7–9%), and from 93 to 101% in rat plasma (CVs, 6.0–7.0%). Precision and accuracy values were within acceptable limits ([18, 21], US Food and Drug Administration. Guidance for industry. Bioanalytical method validation. <http://www.fda.gov/cder/guidance/index.htm>); results are presented in Table 4. Dilution showed no influence on the performance of the method. After a five-fold dilution, precision on the results was <2.0%. The corresponding accuracy values were 90% for EAPB0503 and 98% for EAPB0603.

From human plasma, the mean extraction efficiencies were 85.7% (CV, 5.0%) for EAPB0503, 79.5% (CV, 14.0%) for EAPB0603, and 78.6% (CV, 10.2%) for the internal standard. From rat plasma, they were 91.7% (CV, 6.1%), 72.4% (CV, 10.9%), and 82.3% (CV, 12.0%), respectively. They

Table 3. CVs and recoveries, calculated from back calculated concentrations, from calibration curves performed in rat plasma

Nominal concentrations ($\mu\text{g/L}$)	CV, % (Recovery, %)	
	EAPB0503	EAPB0603
Low calibration curves ($n = 8$)		
Within-day ($n = 6$)		
5	5.4 (96)	11 (93)
7.5	14 (103)	7.9 (100)
10	11 (104)	9.9 (101)
20	2.9 (100)	3.6 (94)
50	4.3 (106)	7.6 (107)
100	4.0 (101)	3.4 (99)
300	3.7 (102)	1.7 (100)
Between-day ($n = 17$)		
5	6.4 (99)	14 (95)
7.5	4.9 (104)	14 (101)
10	5.2 (104)	11 (110)
20	3.2 (102)	3.4 (107)
50	5.8 (102)	4.6 (97)
100	4.0 (103)	7.2 (106)
High calibration curves ($n = 8$)		
Within-day ($n = 6$)		
100	6.4 (99)	14 (95)
150	4.9 (104)	14 (101)
400	5.2 (104)	11 (110)
600	3.2 (102)	3.4 (107)
800	5.8 (102)	4.6 (97)
1000	4.0 (103)	7.2 (106)
Between-day ($n = 17$)		
100	6.4 (99)	14 (95)
150	4.9 (104)	14 (101)
400	5.2 (104)	11 (110)
600	3.2 (102)	3.4 (107)
800	5.8 (102)	4.6 (97)
1000	4.0 (103)	7.2 (106)

were not statistically different over the range of concentrations studied. For both compounds, the lower LOQs were 5 $\mu\text{g/L}$ in the two matrices. These quantitation limits were confirmed by quantifying QC samples at the lower LOQ against a calibration curve; precision was <16% and recovery was 91–111%.

3.3 Stability assays

Stock solutions of EAPB0503, EAPB0603 and internal standard did not reveal any appreciable degradation after 2 months of storage at 4°C.

In human and rat plasma, stored at -80°C , EAPB0503 and EAPB0603 at the concentrations of QC samples were stable for at least 3 months. After bench-top storage at room temperature for 6 h, recoveries were >99% in human plasma and >87% in rat plasma for EAPB0503; and >89% in human plasma and >90% in rat plasma for EAPB0603. At 4°C recoveries were >91% in human and rat plasma for EAPB0503; and >89% in human plasma and >91% in rat plasma for EAPB0603. Reconstituted extracts in the acetonitrile–water–formic acid mixture were stable in the autosampler at 4°C for 48 h. Two freeze–thaw cycles did not affect the stability of EAPB0503 and EAPB0603.

3.4 Pharmacokinetic study

After repeated administrations, the treatment was well tolerated without weight loss or decrease in food and tap water consumed. There were no hematological toxicities or treatment associated deaths.

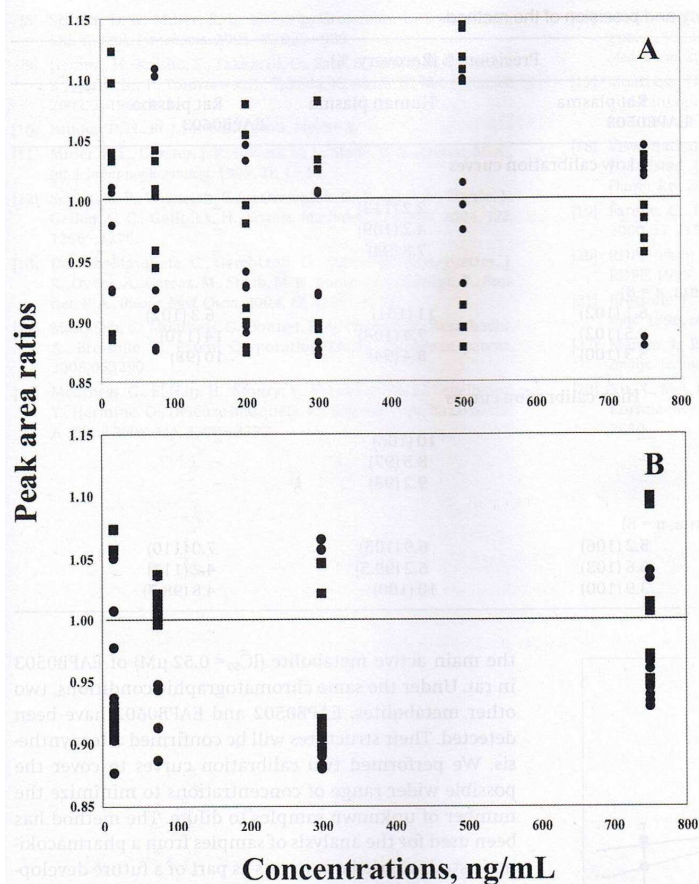


Figure 4. Matrix effect: (A) human plasma; (B) rat plasma. EAPB0503 (●); EAPB0603 (■).

After single intravenous administrations, no side effects were observed. Semilogarithmic plots of the mean (\pm SD) EAPB0503 and EAPB0603 plasma concentration–time profiles are shown in Fig. 5. In rat, EAPB0603 is the main metabolite of EAPB0503. EAPB0603 has *in vitro* cytotoxic activity 2.5 times lower than the parent drug. On the chromatogram presented in Fig. 2C, a second peak with a retention time of 5.8 min was observed at m/z 291. It could correspond to a second metabolite (EAPB0502, 1-(3-methoxyphenyl)imidazo[1,2-*a*]quinoxalin-4-amine) formed from EAPB0503 after loss of the CH_3 moiety on the aminomethyl group. Another metabolite (1-(3-hydroxyphenyl)imidazo[1,2-*a*]quinoxalin-4-amine; EAPB 0602) with a retention time of 3.56 min was detected at m/z 277; it could be formed from the parent drug after loss of the two CH_3 moieties. The structures and a potential activity of these two last metabolites will be confirmed after synthesis. Pharmacokinetic parameters were: i) EAPB0503: total clearance, 2.2 L/h/kg;

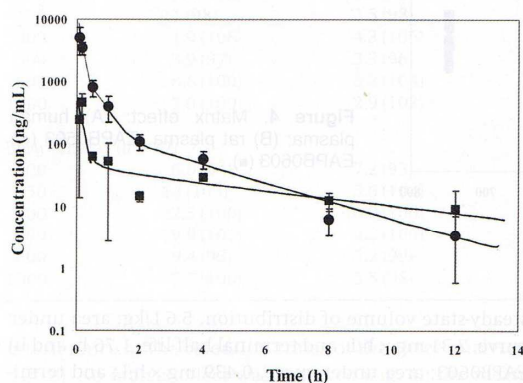
steady-state volume of distribution, 5.6 L/kg; area under curve, $2.31 \text{ mg} \times \text{h/L}$; and terminal half-life, 1.76 h, and ii) EAPB0603: area under curve, $0.439 \text{ mg} \times \text{h/L}$; and terminal half-life, 4.7 h.

4 Discussion and conclusion

We develop imidazo[1,2-*a*]quinoxaline drugs with interesting antitumoral activity against lymphoma [15] and melanoma [16]. On melanoma, the first lead compound (EAPB0203, $\text{IC}_{50} = 1.57 \text{ } \mu\text{M}$) has an *in vitro* activity 110 times higher than fotemustine ($\text{IC}_{50} = 173 \text{ } \mu\text{M}$) and 45 times higher than imiquimod ($\text{IC}_{50} = 70 \text{ } \mu\text{M}$) used as references [16]. In mice model, EAPB0203 is more potent than fotemustine. The structure of EAPB0203 has been modulated and a newly synthesized compound, EAPB0503 ($\text{IC}_{50} = 200 \text{ nM}$), showed *in vitro* cytotoxic activity on melanoma cancer cell line 7–9 times higher than EAPB0203.

Table 4. Within-day and between-day accuracy and precision of the method

Nominal concentrations ($\mu\text{g/L}$)	Precision, % (Recovery, %)			
	Human plasma	Rat plasma EAPB0503	Human plasma	Rat plasma EAPB0603
Low calibration curves				
Within-day ($n = 6$)				
15	2.8 (106)	–	2.2 (113)	–
75	8.7 (101)	–	4.2 (109)	–
200	3.2 (94)	–	7.8 (94)	–
Between-days (human plasma, $n = 17$; rat plasma, $n = 8$)				
15	7.5 (104)	8.1 (102)	11 (101)	6.3 (102)
75	7.1 (92)	8.5 (102)	7.4 (104)	14 (110)
200	7.2 (96)	5.3 (100)	8.4 (94)	10 (98)
High calibration curves				
Within-day ($n = 6$)				
300	6.2 (98)	–	10 (106)	–
500	8.0 (95)	–	8.5 (97)	–
775	5.0 (96)	–	9.2 (98)	–
Between-days (human plasma, $n = 17$; rat plasma, $n = 8$)				
300	6.7 (97)	5.2 (106)	6.9 (105)	7.0 (110)
500	5.9 (98)	6.6 (103)	6.2 (99.5)	4.2 (112)
775	6.0 (98)	3.9 (100)	10 (100)	4.8 (98.7)

**Figure 5.** Mean (\pm SD) plasma concentration versus time curves after a single intravenous (5 mg/kg) administration of EAPB0503 in rat. EAPB0503 (\bullet); EAPB0603 (\blacksquare).

This drug also had interesting *in vitro* activities in other types of tumor (data not shown). In this study, we validated a LC-MS method to quantify EAPB0503 in human and rat plasma. This method involved protein precipitation followed by solid-phase extraction. It has been reported that a protein precipitation procedure prior to solid-phase extraction was the least affected by matrix effects [22, 23]. The LC-MS method described here provides sensitive, accurate, precise, reproducible and relatively fast simultaneous determinations of EAPB0503 and EAPB0603 in rat and human plasma. EAPB0603 is

the main active metabolite ($\text{IC}_{50} = 0.52 \mu\text{M}$) of EAPB0503 in rat. Under the same chromatographic conditions, two other metabolites, EAPB0502 and EAPB0602 have been detected. Their structures will be confirmed after synthesis. We performed two calibration curves to cover the possible wider range of concentrations to minimize the number of unknown samples to dilute. The method has been used for the analysis of samples from a pharmacokinetic study carried out in rats as part of a future development of EAPB0503 and would also be useful in clinical trials at a later stage.

Part of this work was supported by the "Ligue Nationale de Lutte contre le Cancer", Montpellier, France.

The authors declared no conflict of interest.

5 References

- [1] Rudy, S. J., *Dermatol. Nurs.* 2002, 14, 268–270.
- [2] Sauder, D. N., *Br. J. Dermatol.* 2003, 149, 5–8.
- [3] Hengge, U. R., Cusini, M., *Br. J. Dermatol.* 2003, 149, 15–19.
- [4] van Egmond, S., Hoedemaker, C., Sinclair, R., *Int. J. Dermatol.* 2007, 46, 318–319.
- [5] Reiter, M. J., Testerman, T. L., Miller, R. L., Weeks, C. E., Tomai, M. A., *J. Leukoc. Biol.* 1994, 55, 234–240.
- [6] Steinmann, A., Funk, J. O., Schuler, G., Von den Driech, P., *J. Am. Acad. Dermatol.* 2000, 43, 555–556.
- [7] Kang, H. Y., Park, T. J., Jin, S. H., *J. Invest. Dermatol.* 2009, 129, 243–246.

[8] Spaner, D. E., Miller, R. L., Mena, J., Grossman, L., Sorrenti, V., Shi, Y., *Leuk. Lymphoma*. 2005, 46, 935–939.

[9] Hemmi, H., Kaisho, T., Takeuchi, O., Sato, S., Sanjo, H., Hoshino, K., Horiuchi, T., Tomizawa, H., Takeda, K., Akira, S., *Nat. Immunol.* 2002, 3, 196–200.

[10] Sauder, D. N., *Br. J. Dermatol.* 2003, 149, 5–8.

[11] Miller, R. L., Gerster, J. F., Owens, M. L., Slade, H. B., Tomai, M. A., *Int. J. Immunopharmacol.* 1999, 21, 1–14.

[12] Schön, M. P., Wienrich, B. G., Drewniok, C., Bong, A. B., Eberle, J., Geilen, C. C., Gollnick, H., Schön, M., *Invest. Dermatol.* 2004, 122, 1266–1276.

[13] Deleuze-Masquefa, C., Gerebtzoff, G., Subra, G., Fabreguettes, J. R., Owens, A., Carraz, M., Strub, M. P., Bompard, J., George, P., Bonnet, P. A., *Bioorg. Med. Chem.* 2004, 12, 1129–1139.

[14] Masquefa, C., Moarbess, G., Bonnet, P. A., Pinguet, F., Bazarbachi, A., Bressolle, F., Patent Corporation Treaty; European patent, 2008/063290.

[15] Moarbess, G., El-Hajj, H., Kfoury, Y., El-Sabban, M. E., Lepelletier, Y., Hermine, O., Deleuze-Masquefa, C., Bonnet, P. A., Bazarbachi, A., *Blood* 2008, 111, 3770–3777.

[16] Moarbess, G., Deleuze-Masquefa, C., Bonnard, V., Gayraud-Paniagua, S., Vidal, J. R., Bressolle, F., Pinguet, F., Bonnet, P. A., *Bioorg. Med. Chem.* 2008, 16, 6601–6610.

[17] Moarbess, G., Deleuze-Masquefa, C., Khier, S., David, N., Gayraud-Paniagua, S., Bressolle, F., Pinguet, F., Bonnet, P. A., *Eur. J. Med. Chem.* 2009, in press.

[18] Viswanathan, C. T., Bansal, S., Booth, B., DeStefano, A. J., Rose, M. J., Sailstad, J., Shah, V. P., Skelly, J. P., Swann, P. G., Weiner, R., *Pharm. Res.* 2007, 24, 1962–1973.

[19] Farenc, C., Fabreguette, J. R., Bressolle, F., *Comput. Biomed. Res.* 2000, 33, 315–330.

[20] RDPP. Pk-fit computer program, Ver. 2.1, Montpellier, France: RDPP, 1999.

[21] Bressolle, F., Bromet-Petit, M., Audran, M., *J. Chromatogr. B Biomed. Appl.* 1996, 686, 3–10.

[22] Marchi, I., Rudaz, S., Selman, M., Veuthey, J. L., *J. Chromatogr. B Analyt. Technol. Biomed. Life Sci.* 2007, 845, 244–252.

[23] Xu, X., Mei, H., Wang, S., Zhou, Q., Wang, G., Broske, L., Pena, A., Korfmacher, W. A., *Rapid Commun. Mass Spectrom.* 2005, 19, 2643–2650.